Eur Radiol (2004) 14:1275–1284
DOI 10.1007/s00330-004-2267-7

PHYSICS

G. Brix
U. Lechel
R. Veit
R. Truckenbrodt
G. Stamm
E. M. Coppenrath
J. Griebel
H.-D. Nagel

Assessment of a theoretical formalism for dose estimation in CT: an anthropomorphic phantom study

Received: 29 September 2003
Revised: 13 January 2004
Accepted: 21 January 2004
Published online: 19 March 2004
© Springer-Verlag 2004

G. Brix (✉) · U. Lechel · R. Veit
R. Truckenbrodt · J. Griebel
Department of Radiation Protection
and Health, Division of Medical Radiation
Hygiene and Dosimetry,
Federal Office for Radiation Protection,
85764 Neuherberg, Germany
e-mail: gbrix@bfs.de
Tel.: +49-1888-3332300
Fax: +49-1888-3332305

G. Stamm
Department of Radiology,
Hannover Medical School,
Hannover, Germany

E. M. Coppenrath
Department of Radiology,
University of Munich,
Munich, Germany

H.-D. Nagel
Department of Science and Technology,
Philips Medical Systems,
Hamburg, Germany

Abstract Dose assessment in computed tomography (CT) is challenging due to the vast variety of CT scanners and imaging protocols in use. In the present study, the accurateness of a theoretical formalism implemented in the PC program CT-EXPO for dose calculation was evaluated by means of phantom measurements. Phantom measurements were performed with four 1-slice, four 4-slice and two 16-slice spiral CT scanners. Firstly, scanner-specific ${}_nCTDI_w$ values were measured and compared with the corresponding standard values used for dose calculation. Secondly, effective doses were determined for three CT scans (head, chest and pelvis) performed at each of the ten installations from readings of thermoluminescent dosimeters distributed inside an anthropomorphic Alderson phantom and compared with the corresponding dose values computed with CT-EXPO. Differences between standard and individually measured ${}_nCTDI_w$ values were less than 16%. Statistical analysis yielded a highly significant correlation ($P<0.001$) between calculated and measured effective doses. The systematic and random uncertainty of the dose values calculated using standard ${}_nCTDI_w$ values was about –9 and ±11%, respectively. The phantom measurements and model calculations were carried out for a variety of CT scanners and representative scan protocols validate the reliability of the dosimetric formalism considered—at least for patients with a standard body size and a tube voltage of 120 kV selected for the majority of CT scans performed in our study.

Keywords Computed tomography · Patient exposure · Dosimetry · Anthropomorphic phantom · Scanner matching

Introduction

Since its introduction by Hounsfield more than 30 years ago, computed tomography (CT) has made tremendous progress. After the introduction of single-slice spiral CT (SSCT) into clinical practice in 1989 [1], the next considerable advance was the development of multi-slice spiral CT (MSCT) systems a few years ago. The resulting improvement in scanner performance has increased the clinical efficacy of CT procedures and offered promising new applications in diagnostic imaging [2–8].

On the other hand, data from various national surveys have confirmed the growing impact of CT as a major source of patient and man-made population exposure [9]. The levels of the dose for patients undergoing a CT procedure depend in principle on the required image quality and on the extent of the body region to be scanned to meet the specific clinical objectives. In practice, however, numerous factors relating to both the CT scanner and the procedures in use have an influence on the imaging process and thus on patient exposure. Since the effect of these factors on radiation exposure is very complex,

many of those who have to deal with CT in both hospitals and private practices are in general not capable of estimating the relevant quantity for risk assessment—the effective dose—related to the various CT protocols used in their facility and of optimizing scan protocols towards dose reduction.

To overcome this problem, different software packages for dose calculation in CT have been developed [10–15] based on Monte-Carlo data published by the National Radiological Protection Board (NRPB) in the United Kingdom [16] or the Research Center for Environment and Health (GSF) in Germany [17]. One of these software tools—which is widely used because of its flexibility and widespread applicability to nearly all existing SSCT and MSCT scanners—is the dedicated PC program "CT-EXPO" [15]. The algorithm implemented in this program for dose calculation was originally developed and used to analyze data collected in two nationwide surveys on CT practice in Germany performed in 1999 and 2002 [18, 19].

It was therefore the aim of the present study to evaluate the reliability and accurateness of the theoretical formalism implemented in CT-EXPO for dose assessment by means of dose measurements performed at three body regions (head, chest and pelvis) of an anthropomorphic Alderson phantom on a variety of SSCT and MSCT scanners for representative scan protocols.

Materials and methods

Theoretical formalism for dose calculation

The algorithm used for dose calculation has been described in detail elsewhere [20] and is thus only shortly summarized in this subsection.

The calculation of the effective dose E (in mSv) for a single CT scan is based on the equation:

$$E = CTDI_{air} \times \frac{1}{p} \times \sum_{z_L}^{z_U} f(z) \tag{1}$$

with $CTDI_{\mathrm{air}}$ the well-known CT dose index free-in-air (in mGy), i.e., the dose on the axis of rotation of the scanner, and $f(z)$ the scanner-specific conversion factor between $CTDI_{\mathrm{air}}$ and E for a single 10-mm-thick slice placed at the axial position z within the scan region $z_{\mathrm{L}} \le z \le z_{\mathrm{U}}$ in an anthropomorphic model mimicking either a male or female patient. p is the pitch factor defined as the ratio of table movement per gantry rotation and beam collimation $N \times h_{\mathrm{col}}$ with N the number of slices acquired simultaneously and h_{col} the nominal slice (or detector) collimation during data acquisition. For the calculation of the effective dose, tissue weighting factors developed by the ICRP from a reference population of equal numbers of both genders and a wide range of ages were used [21]. In the definition of the effective dose they apply to either gender.

In practice, a convenient assessment of *CTDI* can be made using a pencil ionization chamber with an active length of 100 mm. This measurement is carried out either free-in-air ($CTDI_{\mathrm{air}}$) or—as is usually done—at the center ($CTDI_{100,\mathrm{c}}$) and at the periphery ($CTDI_{100,\mathrm{p}}$) of the standard head or body CT dosimetry phantom [23]. On the assumption that the dose decreases linearly with the radial position from the surface to the center of the phantom, the average dose (in air) can be characterized by the weighted *CTDI*:

$$CTDI_w = \frac{1}{3} CTDI_{100,c} + \frac{2}{3} CTDI_{100,p}. \tag{2}$$

In contrast to this quantity, the normalized weighted *CTDI*:

$$_nCTDI_w = \frac{1}{Q_{el}} \cdot CTDI_w, \tag{3}$$

with Q_{el} the radiographic exposure (in mAs), is—for a given value of the tube voltage and slice collimation—a scanner-specific quantity that comprises the output characteristics of a given type of scanner and thus can be used for further dose assessment. The relation between $CTDI_{\mathrm{w}}$ and $CTDI_{\mathrm{air}}$ depends on the scanner type used for the examination and on the dosimetry phantom considered. For the purpose of dose estimation, the ratio of both quantities is defined for the standard head (H) and body (B) CT dosimetry phantom [22]

$$P_H = \frac{CTDI_{w,H}}{CTDI_{air}} \quad and \quad P_B = \frac{CTDI_{w,B}}{CTDI_{air}}, \tag{4}$$

respectively.

With these definitions, Eq. 1 can be rewritten as:

$$E = \frac{_nCTDI_{w,H/B}}{P_{H/B}} \cdot Q_{el} \cdot \frac{1}{p} \cdot L \cdot f_{mean} \tag{5}$$

with $f_{mean} = \sum f(z)/L$ the scanner-specific average conversion factor over the scan length $L = z_U - z_L$.

Unfortunately, scanner-specific conversion factors are not available for most of the CT scanners and the vast variety of scan parameters applied in clinical routine. Therefore, conversion factors determined for a standard CT scanner ($f_{\mathrm{mean,st}}$) are used and corrected properly. The standard conversion factors $f_{\mathrm{mean,st}}$ are derived from organ-specific conversion factors calculated by Zankl et al. for the anthropomorphic mathematical models ADAM (length of trunk, 70 cm; length of neck and head, 24 cm) and EVA (length of trunk, 66 cm; length of neck and head, 23 cm) by means of Monte-Carlo calculations for the CT scanner SOMATOM DRH (Siemens) working without beam shaping filter at a voltage of U=125 kV and a filtration of 2 mm aluminum and 0.2 mm copper [17, 23]. These calculations take all relevant absorption and scatter processes into account. Corrections are performed according to:

$$f_{mean} = f_{mean,st} \cdot k_{CT} \tag{6}$$

where k_{CT} is a correction factor taking into account differences in scanner geometry, beam filtration and the effect of beam-shaping filters. Correction factors k_{CT} are determined following the concept presented by Shrimpton et al. [24].

Moreover, since for many scanners $_nCTDI_{\mathrm{w,H/B}}$ is not known for all voltages and slice collimations applied in clinical routine, this quantity is calculated from a reference value $_nCTDI_{\mathrm{w,H/B,ref}}$ determined for a voltage U_{ref} and a slice collimation h_{ref} applying appropriate correction factors:

$$_nCTDI_{w,H/B} = _nCTDI_{w,H/B,ref} \cdot k_{OB} \cdot \left(\frac{U}{U_{ref}} \right)^{2.5}. \tag{7}$$

The factor k_{OB}, correcting for differences in slice collimation and for overbeaming effects, is determined analytically using the scanner specifications given in Table 1 according to:

$$k_{OB} = \frac{h_{ref} \cdot (N \cdot h_{col} + dz)}{h_{col} \cdot (N \cdot h_{ref} + dz)}, \tag{8}$$

where dz, the overbeaming parameter, is equal to the width (in z direction) of the rectangle, which is obtained by combining the penumbra triangles at both edges of the dose profile at the detector array.

With these approximations, the effective dose for a CT examination can be calculated according to Eqs. 4–8 on the basis of (1) the scan parameters h_{col}, p, L, Q_{el}, and U used and (2) representa-

Table 1 Summary of characteristic performance parameters[a] for four single-slice and six multi-slice CT systems used for dose calculation in this study

Manufacturer	Scanner	Abbr.	N	U_{ref} (kV)	h_{ref} (mm)	dz (mm)	Head mode			Body mode		
							${}_nCTDI_{w,H}$ (mGy/mAs)	P_H	k_{CT}	${}_nCTDI_{w,B}$ (mGy/mAs)	P_B	k_{CT}
General Electric	LX/i	G-1	1	120	10	0	0.152	0.66	0.80	0.072	0.31	0.65
Philips	Tomoscan AV	P-1	1	120	10	0	0.150	0.75	0.90	0.080	0.40	0.80
Siemens	Somatom Plus 4	S-1	1	120	10	0	0.146	0.82	1.00	0.083	0.47	1.00
Toshiba	XVision	T-1	1	120	10	0	0.162	0.63	0.80	0.065	0.30	0.65
General Electric	Lightspeed QX/i	G-4	4	120	5	3.0/4.0[b]	0.182	0.64	0.80	0.094	0.39	0.80
Philips	Mx8000 Quad	P-4	4	120	5	1.7	0.130	0.75	0.90	0.067	0.39	0.80
Siemens	Volume Zoom	S-4	4	120	5	1.7	0.200	0.76	0.90	0.083	0.49	1.00
Toshiba	Aquilion	T-4	4	120	8	3.0	0.189	0.67	0.80	0.107	0.30	0.65
Philips	Mx8000 IDT	P-16	16	120	1.5	3.0	0.130	0.75	0.90	0.067	0.39	0.80
Siemens	Sensation 16	S-16	16	120	1.5	3.0	0.190	0.76	0.90	0.070	0.41	0.80

[a] Definition of scanner parameters: N, number of simultaneously acquired slices; U_{ref}, reference voltage for ${}_nCTDI_{w,H/B}$; h_{ref}, slice collimation for ${}_nCTDI_{w,H/B}$; dz, width of penumbra; ${}_nCTDI_{w,H/B}$, normalized $CTDI_w$ for head or body mode; $P_{B/H}$, phantom factor for head or body mode; k_{CT}, scanner-specific correction factor.
[b] Value depends on focal spot size.

tive values for $P_{H/B}$, ${}_nCTDI_{w,H/B,ref}$, k_{OB}, k_{CT}, and $f_{mean,st}$ stored in a look-up table characterizing the type of scanner and the body region considered. In the present study, effective doses were first calculated separately for the adult mathematical phantoms ADAM and EVA and were then averaged.

Phantom measurements

To experimentally evaluate the complex dosimetric formalism described, measurements were performed at ten different CT scanners installed in hospitals: four 1-slice, four 4-slice and two 16-slice systems. Table 1 summarizes the manufacturers and models of these scanners along with the scanner-specific parameters used for dose calculation. At each CT installation, two different kinds of phantom measurements were carried out:

Firstly, scanner-type specific ${}_nCTDI_w$ values were determined for both the head and body mode using the reference values U_{ref} and h_{ref} given in Table 1. To this end, a standard head (∅=16 cm) or body (∅=32 cm) CT dosimetry phantom made of PMMA (CT-HB 3216, Wellhöfer, Schwarzenbruck, Germany) was placed on the patient table and positioned exactly in the center of the gantry [20]. CTDI values were measured within both phantoms at the center ($CTDI_{100,c}$) and at four positions at the periphery (1 cm below the surface at 3, 6, 9 and 12 o'clock; $CTDI_{100,p}$) by inserting a pencil-shaped air ionization chamber with an active length of 100 mm (DCT 10, Wellhöfer) into cylindrical holes drilled parallel to the longitudinal axis of the phantoms. The chamber was properly calibrated by a secondary standard dosimeter laboratory for radiation quantities (PTW; Freiburg, Germany). Readings were performed with a dosimeter (Solidose 400 CT, Wellhöfer) connected to the chamber and expressed in terms of air kerma [22]. At each chamber position, dose measurements were repeated between four and six times to reduce the effect of overscanning occurring with some systems and to estimate the standard deviation of $CTDI_{100,c}$ and $CTDI_{100,p}$. Based on this data, the normalized weighted dose index ${}_nCTDI_w$ and the corresponding uncertainty were calculated according to Eqs. 2, 3 and the rules for the propagation of errors [25].

Secondly, dose measurements were performed with an anthropomorphic whole-body Alderson RANDO phantom (Alderson Research Laboratories, Inc., Long Island City, NY) consisting of a human skeleton embedded in plastic material that is radioequivalent to soft tissue (length of trunk, 68 cm; length of neck and head, 23 cm). The phantom is transected into transaxial cross-sections (thickness, 2.5 cm) with holes drilled on a 3-cm×3-cm grid. The holes were plugged either by tissue-equivalent pins or by holder pins for thermoluminescent dosimeters (TLDs). Dose measurements were performed with lithium fluoride (TLD-100; Bicron-Harshaw, Cleveland, OH) rods (size, 1×1×6 mm^3) and chips (size, 3.2×3.2×0.9 mm^3). The TLDs were calibrated for absorbed dose in water using conventional X-ray equipment with a tube potential of 120 kV and a filter of 5 mm aluminum to approximate the radiation quality of CT scanners. This is an appropriate approach since the mass energy absorption coefficient for soft tissues differs by less then 4% from the corresponding value for water at an effective energy of 60 keV [26]. (The resulting error in the dose estimated for bone surface can be neglected, because this quantity contributes to the effective dose only with a tissue weighting factor of w_T=0.01). Individual calibration, annealing and read-out of the TLDs were performed following a standard procedure [27]. Reading of individual TLDs did not differ by more than 3% from the mean value of the complete group consisting of several hundred chips and rods, when irradiated under the some exposure conditions. For each measurement at the Alderson phantom, 100 TLD rods were suitably distributed inside and more than 83 TLD chips at the surface of the phantom to sample the non-uniform dose distribution.

To determine the position of the TLDs in the Alderson phantom for dose assessment in the relevant tissues and organs, digital images of gross anatomical sections of the "visible human" [28] were matched to the size of the 36 transaxial cross-sections of the Alderson phantom using structures of the skeleton as landmarks. The size and position of the relevant organs were then transferred to transparent paper, which was fixed on the corresponding phantom sections. For smaller organs, equivalent doses were obtained by taking the mean of the dose values recorded by the TLDs within the specified organs. In contrast, equivalent doses for extended organs (lung, skin, bone and red bone marrow) were estimated using specific weighting factors for the various cross-sections of the Alderson phantom similar to the approach presented by Huda and Sandison [29]. Finally, the effective dose E was calculated from the tissue and organ equivalent doses using the above-mentioned ICRP-60 tissue weighting factors.

At each CT installation, three different body regions of the Alderson phantom (head, chest and pelvis) were scanned applying typical protocols of the particular hospital. The scan parameters of the 30 CT examinations carried out are given in Table 2 along

Table 2 Summary of scan parameters used at ten spiral CT systems for the examination of the head, chest and pelvic region of the Alderson phantom

Region	Scanner[a]	Scan parameters[b]					Position[c]	Effective doses	
		U (kV)	Q_{el} (mAs)	h_{col} (mm)	p	L (cm)		E_{calc} (mSv)	$E_{Alderson}$ (mSv)
Head[d]	G-1	120	300	3/7	1.0	13.5	3/4	1.6	1.7
	P-1	120	500/400	3/7	1.66/1.43	13.8	3/4	1.4	1.4/1.4[e]
	S-1	120	278	2/8	1.0	15.0	3/4	1.6	1.6
	T-1	130/120	450/250	5/7	1.0	13.1	3/4	1.8	2.0
	G-4	120	200	4×5	0.75	15.0	3/4	1.9	2.0
	P-4	120	219	4×2.5	0.875	15.0	3/4	1.3	1.5
	S-4	120	182	4×2.5	0.65	14.3	3/4	2.2	2.5
	T-4	120	300	4×2	1.375	14.3	3/4	1.9	2.2
	P-16	120	365	16×0.75	1.0	14.4	3/4	1.9	2.1
	S-16	120	191	16×1.5	0.425	14.8	3/4	3.1	3.7
Chest	G-1	140	120	7	1.5	29.1	15	4.0	3.9
	P-1	120	175	7	1.43	27.0	15	4.1	3.7
	S-1	120	150	5	1.5	27.8	15/16	3.8	3.3
	T-1	120	200	7	1.43	28.0	14/15	4.3	4.7
	G-4	120	104	4×5	1.5	27.8	15	2.8	3.8
	P-4	120	87.5	4×2.5	0.875	27.3	14/15	3.1	3.9
	S-4	120	56.3	4×2.5	0.75	27.2	15	2.8	2.7
	T-4	120	100	4×5	0.75	30.0	14	7.6	8.0
	P-16	120	81	16×0.75	0.9	32.0	15/16	3.5	4.3
	S-16	120	120	16×1.5	1.0	30.0	15/16	4.0	4.9
Pelvis	G-1	120	160	7	1.5	22.8	30	3.3	3.5
	P-1	120	200	5	1.4	19.2	31	4.1	3.8
	S-1	120	165	8	1.5	20.4	30/31	3.6	3.2
	T-1	120	200	10	1.5	20.7	30/31	3.6	3.9
	G-4	120	200	4×5	1.5	19.5	30/31	4.7	5.5
	P-4	120	225	4×5	0.625	26.3	30	12.8	15.6
	S-4	120	124	4×2.5	0.75	19.5	30/31	5.4	5.2/5.4[e]
	T-4	120	125	4×5	0.75	19.5	31	8.3	10.7
	P-16	120	135	16×0.75	0.9	19.9	30/31	4.3	4.5
	S-16	120	160	16×1.5	1.0	20.0	30/31	4.1	4.4

For each examination, the effective dose calculated using the scanner-specific ${}_nCTDI_w$ values summarized in Table 1 is given along with the corresponding value determined from TLD measurements at the Alderson phantom. The scan parameters are typical for the facilities at which the CT measurements were performed and are not necessarily recommended by the manufacturers.

[a] Abbreviations are defined in Table 1.

[b] Definition of scan parameters: U, tube voltage; Q_{el}, electrical current-time product; h_{col}, slice collimation; p, pitch; L, scan length.

[c] Number of cross-section(s) of the Alderson phantom, the middle of which was positioned at the axial center of the CT system.

[d] Head examinations were carried out at SSCT scanners with different protocols for cerebellum/cranial base and upper brain.

[e] Result of repeat measurement.

with the number(s) of the cross-section(s) of the Alderson phantom, the middle of which was at the center of the scanned regions. In order to estimate the uncertainty in the effective doses derived from the TLD measurements at the Alderson phantom, two measurements (head region at the scanner P-1 and pelvic region at the scanner S-4) were repeated after some weeks. Furthermore, for each of the 30 examinations performed at the Alderson phantom, the effective dose was computed with CT-EXPO (version V1.3, Hamburg/Hannover, Germany; module "calculate") using both the standard ${}_nCTDI_w$ values tabulated in the program (cf. Table 1) and the ${}_nCTDI_w$ values measured at the particular scanner.

Correlation and error analysis

Statistical comparisons were performed using the program package SigmaStat (version 2.03; SPSS Science Software, Erkrath, Germany). Correlation between random variables X and Y was tested at a significance level of P=0.05 by calculating Spearman's rank correlation coefficient r_S.

To quantify the functional relationship between two random variables X and Y for which a sample of N pairs of data (x_n, y_n) is available (such as measured and standard ${}_nCTDI_w$ values or measured and calculated effective doses), a regression line through the origin was computed by the method of weighted least squares. According to this approach, the best estimate for the slope α of the regression line is:

$$\alpha = \sum_{n=1}^{N} w_n x_n y_n \Big/ \sum_{n=1}^{N} w_n x_n^2 \qquad (9)$$

where the weighting factors $w_n=1/\sigma_n^2$ are defined by the unequal uncertainties σ_n in the dependent data y_n [25]. To analyze the relationship between measured and standard ${}_nCTDI_w$ values, a constant error model was assumed, which means that the uncertainty in the data can be approximated by an error term with an unknown but constant variance. Contrarily, a linear error model was used for the analysis of the calculated effective doses, i.e., $\sigma_n = \delta_y(\alpha x_n) \approx \delta_y y_n$, where δ_y defines the relative uncertainty. The adequacy of these idealized error models was tested by a residual analysis of the sample data.

The relative *systematic* deviation between the two variables X and Y is given by:

$$\varepsilon = \alpha - 1 \tag{10}$$

whereas the *random* uncertainty in the dependent variable Y, which characterizes the spread of the sample data around the fitted regression line, is given by

$$\sigma_y = \sqrt{\frac{1}{N-1}\sum_{n=1}^{N}(y_n - \alpha x_n)^2} \quad \textit{and}$$
$$\delta_y = \sqrt{\frac{1}{N-1}\sum_{n=1}^{N}\left(\frac{y_n - \alpha x_n}{\alpha x_n}\right)^2} \tag{11}$$

for the constant and the linear error model, respectively. It should be noted that these formulas are derived under the assumption that the random uncertainty in the independent variable X can be neglected with respect to those in the dependent variable Y. Whereas this was an adequate approximation for error analysis of the calculated dose values because $(\delta_{E,\,\mathrm{Alderson}}/\delta_{E,\,\mathrm{calc}})^2 \ll 1$ (see below), the uncertainty in the measured ${}_nCTDI_{\mathrm{w}}$ values could not be neglected in comparison with the uncertainty in the corresponding standard values. Since the uncertainties in the random variables X and Y are independent in the latter case, an effective uncertainty in the dependent variable Y

$$\hat{\sigma}_y = \sqrt{\sigma_y^2 + (\alpha\sigma_x)^2} \tag{12}$$

was estimated, where σ_x is the random uncertainty in the variable X [25].

Results

As described above, dose assessment in CT is based on scanner-specific ${}_nCTDI_{\mathrm{w}}$ values. For the 10 CT scanners investigated in this study, the measured ${}_nCTDI_{\mathrm{w}}$ values are presented in Fig. 1a,b for the body and head mode compared to the corresponding standard values used in the software package. Uncertainties in the measured ${}_nCTDI_{\mathrm{w}}$ values were dominated by systematic differences in the dose values determined at the four peripheral phantom positions due to a varying influence of table attenuation and overscanning. The average error in the measured values was σ_{CTDI}=0.006 mGy/mAs. Differences between standard and individually measured ${}_nCTDI_{\mathrm{w}}$ values were less than 16%. Statistical analysis demonstrated a highly significant correlation between measured and standard ${}_nCTDI_{\mathrm{w}}$ values (P<0.001, r_S=0.940, α=1.023). According to Eqs. 10, 12, a linear regression analysis (Fig. 1c) yielded a systematic error in the standard ${}_nCTDI_{\mathrm{w}}$ values used for dose calculation of $\varepsilon_{\mathrm{CTDI}}$=+2.3% and a random uncertainty of $\hat{\sigma}_{CTDI} = 0.010$ mGy/mAs.

Figure 2 shows, as a representative example, the position of the three body regions within the Alderson phantom scanned with a 4-slice CT scanner. The corresponding "pelvic region" of the mathematical model ADAM defined for dose calculation is indicated in Fig. 3. Comparison of the images presented in Figs. 2, 3 reveals a substantial source of error in CT dosimetry and thus in our study design: although the size of the anthropomorphic Alderson phantom lies exactly between that of the mathematical models ADAM and EVA, the two models

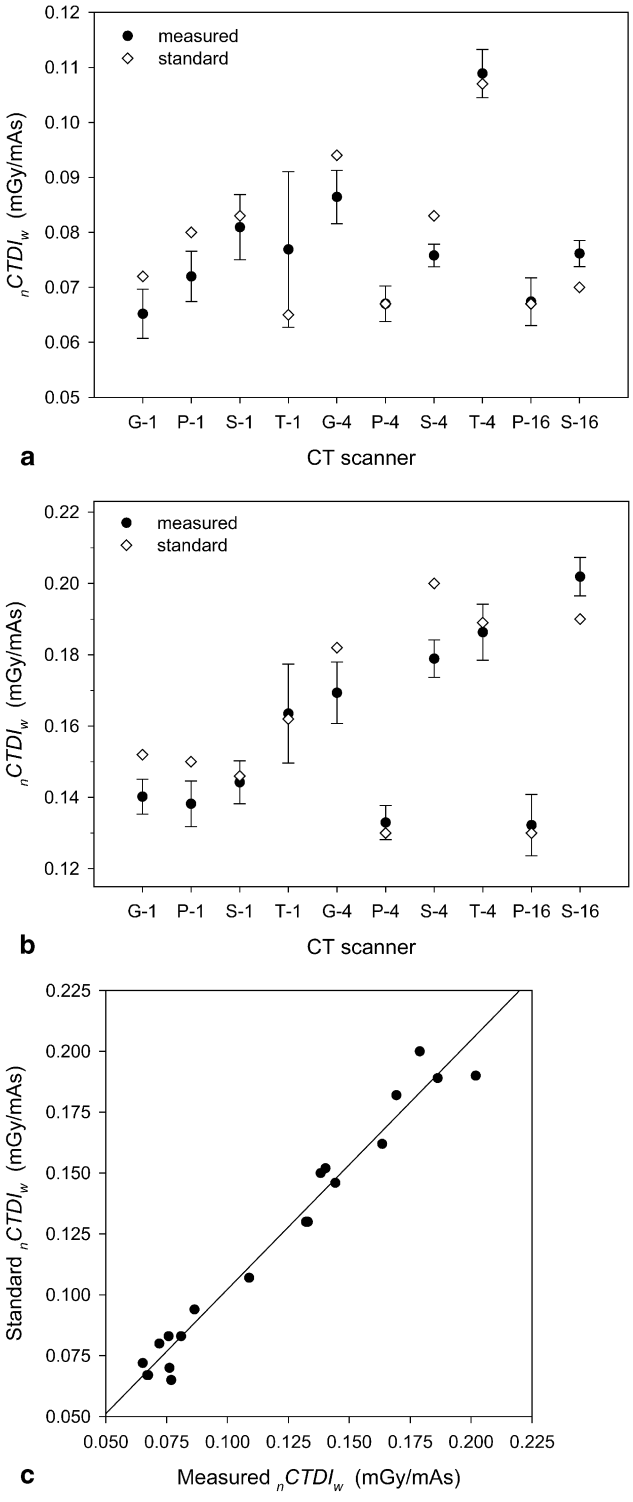

Fig. 1 Assessment of the standard ${}_nCTDI_{\mathrm{w}}$ values used for dose calculation for the 10 CT systems listed in Table 1. Scanner-specific comparison of standard with individually measured (mean ± standard deviation) ${}_nCTDI_{\mathrm{w}}$ values for **a** the body and **b** head mode. **c** Linear least squares fit through the origin of both the body and head mode data. Please note that two data points overlap

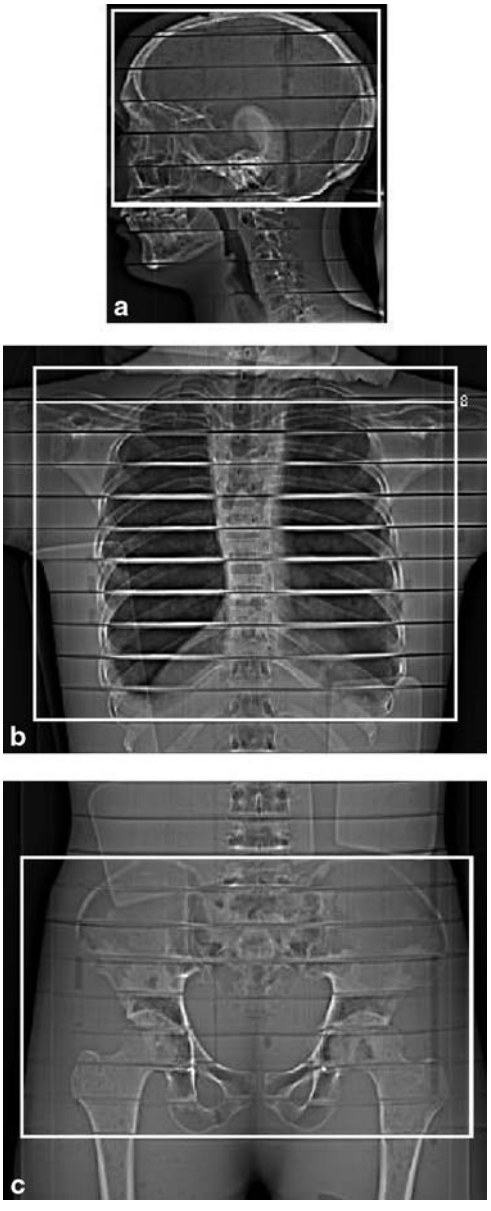

Fig. 2 Position of the three partial-body regions within the anthropomorphic Alderson phantom scanned at a 4-slice CT scanner (S-4). **a** Sagittal scout of the head, **b** coronal scout of the chest and **c** coronal scout of the pelvic region

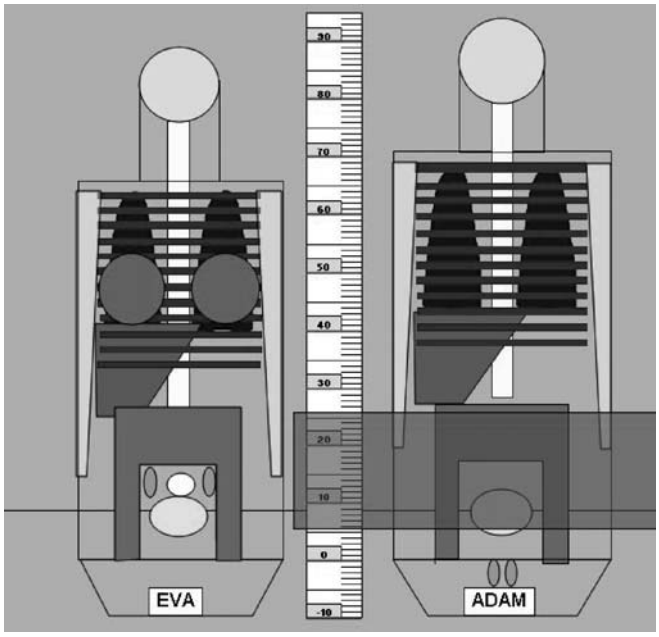

Fig. 3 Size and internal configuration of the anthropomorphic mathematical models EVA (*left*) and ADAM (*right*) used for dose calculation. The partial-body region marked corresponds to the region within the Alderson phantom shown in Fig. 2c

and phantoms have a rather different internal configuration. As a consequence, tissues and organs with different tissue weighting factors may be partly in the scan region of the phantom, but not of the model or vice versa.

The effective doses calculated for the 30 CT procedures summarized in Table 2 are plotted in Fig. 4 vs. the corresponding dose values determined experimentally on the basis of TLD measurements at the Alderson phantom. Repetition of the TLD measurement at the head and chest region of the Alderson phantom after some weeks at two different scanners resulted in a difference in the determined effective doses of less than 4% ($\delta_{E,\,\mathrm{Alderson}} \approx 4\%$). Deviations between calculated and measured doses were less than 32% for the sample data. Statistical evaluation indicated that the use of standard ${}_nCTDI_{\mathrm{w}}$ values (Fig. 4a; $P<0.001$, $r_S=0.931$, $\alpha=0.912$) does result only in a slightly inferior correlation between calculated and measured effective doses than the use of the individually measured ${}_nCTDI_{\mathrm{w}}$ values (Fig. 4b; $P<0.001$, $r_S=0.950$, $\alpha=0.909$). From the two regression lines shown in Fig. 4a,b, the following partitioning of the total uncertainty into a systematic and random component was derived: $\varepsilon_E^{\mathrm{standard}} = -8.8\%$, $\delta_E^{\mathrm{standard}} = 11.3\%$ and $\varepsilon_E^{\mathrm{individual}} = -9.1\%$, $\delta_E^{\mathrm{individual}} = 10.5\%$. It should be noted that for a given CT examination the calculated and the measured effective dose ($E_{calc}^{individual} = 0.010$ and E_{Alderson}, respectively) is directly proportional to the radiographic exposure chosen for the scan and the individually measured ${}_nCTDI_{\mathrm{w}}$ value. Due to this fact, the estimated uncertainties $\varepsilon_E^{\mathrm{individual}} \equiv \varepsilon_{\mathrm{calc}}$ and $\delta_E^{\mathrm{individual}} \equiv \delta_{\mathrm{calc}}$ are independent from these parameters (cf. Eqs. 10, 11) and thus reflect the reliability of the corrections performed by the calculation algorithm according to Eqs. 6, 7, 8 and the accurateness with which the anthropomorphic mathematical models ADAM and EVA approximate the human body or (in our investigation) the Alderson phantom. The same holds true for the ratio $R_E = E_{calc}^{individual} / E_{Alderson}$, which is plotted in Fig. 5 for each of the 30 CT examinations performed. Whereas the ratios calculated for the four SSCT scanners are dis-

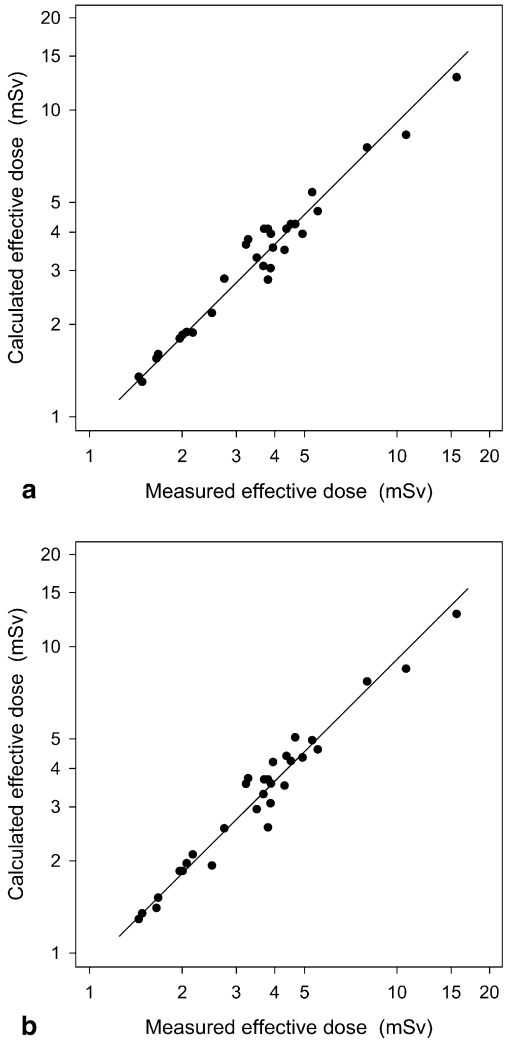

Fig. 4 The statistical relation between calculated and measured effective doses for CT examinations of the head, chest and pelvic region carried out at ten different CT systems (cf. Table 1) using facility-specific scan protocols (cf. Table 2). Dose calculation was performed with **a** the standard ${}_nCTDI_w$ values listed in Table 1 and **b** the individual ${}_nCTDI_w$ values measured with each scanner (cf. Fig. 1). The *solid lines* give the result of a weighted least squares fit through the origin

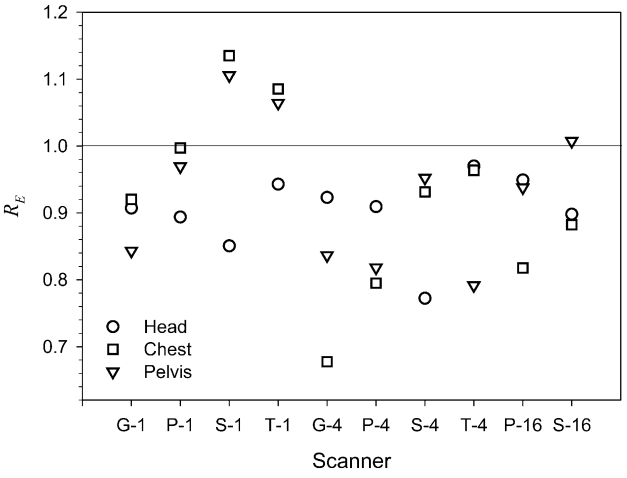

Fig. 5 Ratio $R_E = E_{calc}^{individual}/E_{Alderson}$ computed for the 30 CT measurements summarized in Table 2. The data characterize the reliability of the various corrections performed in the dosimetric formalism and the accurateness with which the anthropomorphic mathematical models ADAM and EVA approximate the Alderson phantom (cf. Figs. 2, 3)

tributed around the nominal value of R_E=1, the ratios for the six MSCT scanners are consistently too low.

To estimate exposure to the embryo from a CT examination of a female patient conducted (unintentionally) in the very early stages of pregnancy, the uterine dose is often used as a surrogate. The uterine doses calculated for the female anthropomorphic mathematical model EVA using both the standard and individually measured ${}_nCTDI_w$ values for the 10 CT examinations of the pelvic region are plotted in Fig. 6 vs. the corresponding uterine doses determined from the TLD measurements at the Alderson phantom. The dosimetric formalism overestimates the uterine dose by about 25% in average, when standard ${}_nCTDI_w$ values are used for dose calculation.

Discussion

The major challenge in assessing radiation exposure of patients undergoing a CT procedure is the vast variety of CT scanners and imaging protocols in use at both hospitals and private practices. In the dosimetric formalism investigated in the present study, dose calculation is performed on the basis of actual scan parameters together with representative correction factors characterizing the type of CT scanner used and the body region irradiated. A similar approach of CT scanner matching is used for dose assessment by the NRPB and the Medical Devices Agency group on "Imaging Performance Assessment of CT Scanners (ImPACT)" [11, 30].

The basic quantity for dose assessment is the scanner-specific normalized weighted CT dose index ${}_nCTDI_w$, which comprises the output characteristics of a given type of scanner. Standard values for this quantity are provided by the manufacturers with the specification that the values determined at individual scanners of the particular scanner model do not differ by more than ±20%. This could be verified by our phantom measurements at ten different types of CT scanners, which yielded a maximum deviation between standard and measured ${}_nCTDI_w$ values of 12 and 16% for the head and body mode, respectively. (Note: the scanner-specific ${}_nCTDI_w$ values used for dose calculation in the software package CT-EXPO are not always identical to those indicated at the CT console).

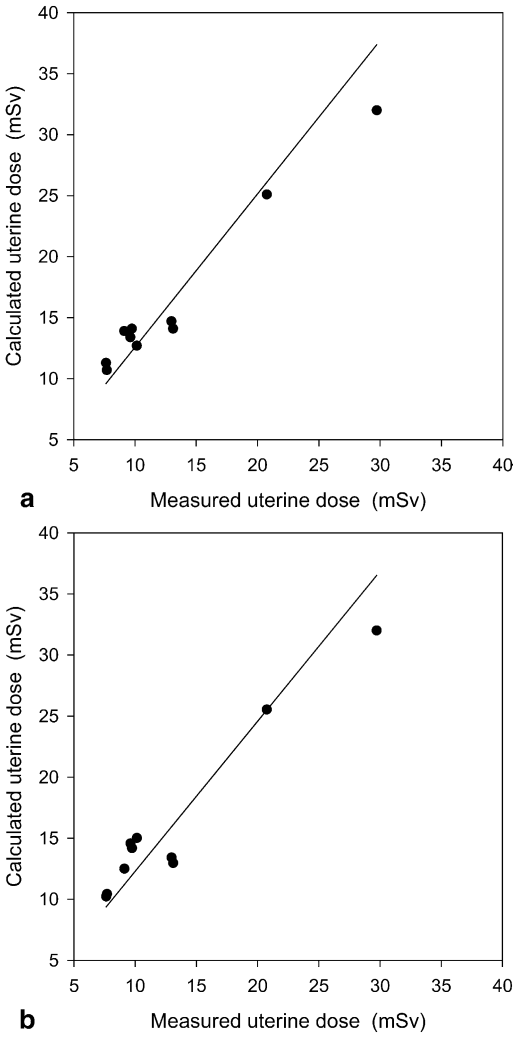

Fig. 6 Statistical relation between calculated and measured uterine doses determined for ten CT examinations of the pelvic region carried out at different CT systems (cf. Table 1), using facility-specific scan protocols (cf. Table 2). Dose calculation was performed with **a** the standard ${}_nCTDI_w$ values summarized in Table 1 and **b** the individual ${}_nCTDI_w$ values measured at each scanner (cf. Fig. 1). The *solid lines* give the result of a weighted least squares fit through the origin

The relevant quantity for risk assessment and optimization of examination protocols is the effective dose, which depends not only on the CT scanner and the scan parameters used, but also on the body region examined. To evaluate the accurateness of dose estimation using the dosimetric formalism under consideration, measurements were performed with the anthropomorphic whole-body Alderson phantom with ten different CT scanners. The range and complexity of the performance evaluation was further increased by using typical scan protocols of the hospitals involved for the examination of the head, chest and pelvis instead of predefined standard protocols. Thus, 30 different measurements were carried out in total, representing a wide range of radiographic exposures, beam filtration, beam shaping filters, scanner geometries, overbeaming parameters, slice collimations and pitch factors. Nevertheless, statistical analysis yielded a highly significant correlation ($P<0.001$) between computed and measured effective doses, regardless of whether the standard or the individually measured ${}_nCTDI_w$ values were used for dose calculation. As compared to the TLD measurements, however, calculated effective doses were systematically lower by about 9%.

Figure 5 reveals that systematic differences are generally larger for MSCT as compared to SSCT scanners. This is partially due to the fact that the dosimetric algorithm neglects the effect of "overranging." This effect results from the need to acquire data from above and below the actual scan volume for data interpolation. To which extent the length of the scan is increased depends on various factors, which are often not obvious. At least, overranging is determined by the total collimation, $N \cdot h_{col}$, and the pitch factor. It should also depend on whether a 180 or 360°-type interpolation algorithm is used. Overranging is more pronounced with MSCT scanners when wide collimations, such as 4×5 mm or 16×1.5 mm, are used, which are markedly larger than the slice collimations employed by SSCT scanners [31]. For the types of MSCT scanners and scan protocols considered in this study, the systematic error due to overranging should typically be less than 5% and should not exceed 10%. Another simplification, which should be taken into account, is the kind of scanner matching employed in the software. As mentioned above, scanner matching is achieved via the scanner factors k_{CT}, which are arranged in steps of up to 20%. Consequently, "random" errors in the order of up to ±10% may occur.

Since CT examinations on pregnant patients also result in an exposure to the unborn, they are not carried out routinely without overriding clinical indications. Nevertheless, inadvertent exposure to the embryo from a CT examination conducted in the very early stages of pregnancy may occur [9]. Figure 6 provides evidence that the dosimetric formalism under investigation gives conservative estimates of the uterine dose, which is often used as a surrogate for the embryonal dose.

The description of the dosimetric formalism presented in this paper reveals that there are two major sources of uncertainties: Firstly, uncertainties in the standard ${}_nCTDI_w$ values (systematic component, +2.3%; random component, 0.010 mGy/mAs) and, secondly, errors caused (1) by the correction algorithms described by Eqs. 6, 7, 8, (2) by the crude approximation of the human body (respective: the Alderson phantom) by the anthropomorphic mathematical models ADAM and EVA (cf. Figs. 2, 3) and (3) by the resultant uncertainties in the definition of the scan region in the mathematical models. Based on the sample data presented in Fig. 4b, the uncertainty introduced by the three latter mentioned

effects can be divided into a systematic and a random component of –9.1% and ±10.5%, respectively. On the reasonable assumption that the two major sources of random errors discussed are independent with respect to the CT examination of an individual patient at any scanner of a particular model, the resulting relative random uncertainty in the effective doses derived from the standard ${}_nCTDI_w$ values is $\sqrt{\delta_{calc}^2 + (\hat{\sigma}_{CTDI}/{}_nCTDI_w)^2}$ [25]. For an average ${}_nCTDI_w$ value of 0.120 mGy/mAs, this formula gives an uncertainty of 13.4%, which agrees quite well with the random uncertainty of $\delta_{calc}^{standard} = 11.3\%$ derived directly from the regression analysis shown in Fig. 4a. However, it should be mentioned that the presented error analysis holds only for patients with a body size similar to that of the Alderson phantom or of the mathematical models ADAM and EVA.

In the future, a substantial advance in dose assessment of patients undergoing a CT examination may be reached by using voxel models, which tend to cover individual anatomies, as the basis for numerical dosimetry by means of Monte-Carlo simulations, instead of crude mathematical models that approximate the complex anatomy of the human body only very roughly. At present, two pediatric and five adult voxel phantoms of both sexes, different ages and stature have been derived from high-resolution CT or MR images [32].

Finally, a limitation of the methodological approach used in the present study should be mentioned: the evaluation of the dosimetric formalism described is based on a comparison of effective doses calculated and measured for scan protocols frequently used for patient examinations in ten different hospitals. Despite this variety of users, however, nearly all measurements were performed with a tube voltage of 120 kV. One thus cannot rule out the possibility that somewhat larger errors in the calculated dose values may occur when scans are carried out with much lower or higher tube voltages (e.g., 80 or 140 kV).

From a radiation hygienic point of view, the large differences in the effective doses determined for the various examination protocols are striking. For example, there is a factor of nearly five between the lowest and highest effective dose determined for CT scans of the pelvis. This, however, is of no relevance for the present study, since we did not investigate image quality in relation to patient exposure, but rather compare measured and calculated effective doses for protocols currently in use. A reduction of radiation exposure to patients may be achieved in the future due to the establishment and use of diagnostic reference levels and the use of low-dose scan protocols for a variety of clinical examinations [33–36].

In conclusion, the phantom measurements and model calculations performed in this study for a variety of scanners validate the reliability and accurateness of the dosimetric formalism described—at least for CT protocols frequently used in clinical routine. Error analysis yielded a systematic and random uncertainty of about –9 and ±11%, respectively, for the effective doses calculated using standard ${}_nCTDI_w$ values. Beyond the actual scope of the present investigation, the extensive TLD measurements with the Alderson phantom that are reported can also serve as a reference data set for the evaluation of alternative approaches for dose assessment in CT. To this end, the relevant scanning parameters are summarized in detail for each of the 30 CT scans carried out along with the corresponding effective dose and the length and center of the scan region within the Alderson phantom.

Acknowledgements The authors would like to thank the owners and the staff of the ten facilities where the phantom measurements were performed for their excellent collaboration. Furthermore, the support of R. Banckwitz and C. Süß (Siemens AG, Medical Solutions, Forchheim, Germany) is gratefully acknowledged.

References

1. Kalender WA, Seissler W, Klotz E, Vock O (1990) Spiral volumetric CT with single-breath-hold technique, continuous transport, and scanner rotation. Radiology 176:181–183
2. Berland LL, Smith JK (1998) Multidetector-array CT: once again, technology creates new opportunities. Radiology 209:327–329
3. Klingenbeck-Regn K, Schaller S, Flohr T, Ohnesorge B, Kopp AF, Baum U (1999) Subsecond multi-slice computed tomography: basics and applications. Eur J Radiol 31:110–124
4. Rydberg J, Buckalter KA, Caldemeyer KS, Phillips MD, Conces DJ, Aisen AM, Persohn SA, Kopecky KK (2000) Multisection CT: scanning techniques and clinical applications. Radiographics 20:1787–1806
5. Dawson P, Lees WR (2001) Multi-slice technology in computed tomography. Clin Radiol 56:302–309
6. Laghi A, Lannaccone R, Panebianco V, Carbone L, Passariello R (2001) Multislice CT colonography: technical developments. Semin Ultrasound CT MR 22:425–431
7. Schoepf UJ, Becker CR, Hofmann LK, Das M, Flohr T, Ohnesorg BM, Baumert B, Rolnick J, Alles JM, Raptopulos V (2003) Multislice CT angiography. Eur Radiol 13:1946–1961
8. Hong C, Becker CR, Schoepf UJ, Ohnesorge B, Bruening R, Reiser MF (2002) Coronary artery calcium: absolute quantification in nonenhanced and contrast-enhanced multi-detector row CT studies. Radiology 223:474–480
9. UNSCEAR 2000 Report, vol. I, sources and effects of ionizing radiation. Annex D: medical radiation exposures (2000). United Nations Sales Publications
10. LeHeron JC (1993) CTDOSE—a computer program to enable the calculation of organ doses and dose indices for CT examinations. Ministry of Health, National Radiation Laboratory, Christchurch, New Zealand

11. Imaging Performance Assessment of CT-Scanners Group. ImPACT CT Patient Dosimetry Calculator v. 0.99 j. London: ImPACT. http://www.impactscan.org
12. Kalender WA, Schmidt B, Zankl M, Schmidt M (1999) A PC program for estimating organ dose and effective dose values in computed tomography. Eur Radiol 9:555–562
13. National Institute of Radiation Hygiene (1999) CT dose calculation software "CT-Dose". National Institute of Radiation Hygiene, Herlev. ctdose@sis.dk
14. Tack D (2001) Comments on Kalender et al.: a PC program for estimating organ dose and effective dose values in computed tomography. Eur Radiol 11:2641–2642 and Kalender WA, Schmidt B (2001) Reply to Tack D: a PC program for estimating organ dose and effective dose values in computed tomography. Eur Radiol 11:2643
15. Stamm G, Nagel HD (2002) CT-Expo-ein neuartiges Programm zur Dosisevaluierung in der CT. Fortschr Rontgenstr 174:1570–1576
16. Jones DG, Shrimpton PC (1991) Survey of CT practice in the UK. Part 3. Normalised organ doses calculated using Monte Carlo techniques. NRPB-250. National Radiological Protection Board, Oxon
17. Zankl M, Panzer W, Drexler G (1991) The calculation of dose from external photon exposures using reference human phantoms and Monte Carlo methods. Part IV. Organ doses from tomographic examinations. GSF report 30/91. Neuherberg
18. Galanski M, Nagel HD, Stamm G (2001) CT-Expositionspraxis in der Bundesrepublik Deutschland. Fortschr Rontgenstr 173:R1–R66
19. Brix G, Nagel HD, Stamm G, Veit R, Lechel U, Griebel J, Galanski M (2003) Radiation exposure in multi-slice versus single-slice spiral CT: Results of a nationwide survey. Eur Radiol 13:1979–1991
20. Nagel HD, Galanski M, Hidajat N, Maier W, Schmidt T (2002) Radiation exposure in computed tomography–fundamentals, influencing parameters, dose assessment, optimisation, scanner data, terminology. 4th edn. CTB Publications, Hamburg (ctb-publications@gmx.de)
21. ICRP Publication 60 (1991) 1990 recommendations of the International Commission on Radiological Protection. Annals of the ICRP vol 21/1-3. Elsevier Science, Oxford
22. European Commission (1999) Report EUR 16262 EN "European guidelines on quality criteria for computed tomography"
23. Kramer R, Zankl M, Wiliams G, Drexler G (1982) The calculation of dose from external photon exposures using reference human phantoms and Monte Carlo methods. Part I. The male (Adam) and female (Eva) adult mathematical phantoms. GSF report S-885. Neuherberg
24. Shrimpton PC, Jones DG, Hillier MC, Wall BF, Leheron JC, Faulkner K (1991) Survey of CT practice in the UK. Part 2. Dosimetric aspects. NRPB-249. London: HMSO, 48
25. Taylor JR (1997) An introduction to error analysis: The study of uncertainties in physical measurements. 2nd edn. University Science Books, Sausalito, CA
26. ICRU Publication 17 (1970) Radiation dosimetry: X-rays generated at potentials of 5 to 150 kV. ICRU Publications, Washington, DC
27. European Commission (2000) Report EUR 19604 EN "Recommendations for patient dosimetry in diagnostic radiology using TLD"
28. Jastrow W Atlas of human sections in the internet. Labelling of sections from the visible human project. http://www.uni-mainz.de/FB/medizin/anatomie/workshop/engl/welcome.html
29. Huda W, Sandison GA (1984) Estimation of mean organ doses in diagnostic radiology from Rando phantom measurements. Health Phys 47:463–467
30. Shrimpton PC, Edyvean S (1998) CT scaner dosimetry. Br J Radiol 71:1–3
31. Cohnen M, Poll LW, Puettmann C, Ewen K, Saleh A, Mödder U (2003) Effective doses in standard protocols for multi-slice CT scanning. Eur Radiol 13:1148–1153
32. Petoussi-Henss N, Zankl M, Fill U, Regulla D (2002) The GSF family of voxel phantoms. Phys Med Biol 47:89–106
33. Dinkel HP, Sonnenschein M, Hoppe H, Vock P (2003) Low-dose multislice CT of the thorax in follow-up of malignant lymphoma and extrapulmonary primary tumors. Eur Radiol 13:1241–1249
34. Iannaccone R, Laghi A, Catalano C, Mangiapane F, Piacentini F, Passariello R (2003) Feasibility of ultra-low-dose multislice CT colonography for the detection of colorectal lesions: preliminary experience. Eur Radiol 13:1297–1313
35. Diederich S (2003) Radiation dose in helical CT for detection of pulmonary embolism. Eur Radiol 13:1491–1493
36. Jakobs TF, Wintersperger BJ, Herzog P, Flohr T, Suess C, Knez A, Reiser MF, Becker CR (2003) Ulta-low-dose coronary artery calcium screening using mutlislice CT with retrospective ECG gating. Eur Radiol 13:1923–1930